Received: 2 December 2022 | Revised: 21 March 2023 | Accepted: 13 April 2023

DOI: 10.1002/cta.3642

BRIEF REPORT

WILEY

A low-cost fault-tolerant permanent magnet brush-less direct current motor drive for low-power electric vehicle applications

Patnana Hema Kumar[1,2] | **Suresh Lakhimsetty**[3] | **Veeramraju Tirumala Somasekhar**[1]

[1]Department of Electrical Engineering, National Institute of Technology Warangal, Warangal, Telangana, India

[2]Advanced Engineering Team of Hella India Automotive Private limited, Pune, India

[3]Department of Electrical Engineering, Sardar Vallabhbhai National Institute of Technology Surat, Surat, Gujarat, India

Correspondence
Patnana Hema Kumar, Department of Electrical Engineering, National Institute of Technology Warangal, Warangal, TS 506004, India; and Advanced Engineering Team of Hella India Automotive Private limited, Pune, India.
Email: hema1729@student.nitw.ac.in

Summary

This paper proposes a fault-tolerant power converter for a voltage source inverter (VSI)-driven permanent magnet brush-less direct current (PM-BLDC) motor drive, which is suitable for low-power electric vehicle (EV) applications. With the proposed topology, it is possible to deliver rated power to the PM-BLDC motor even after the incidence of either an open-circuit fault (OCF) or a short-circuit fault (SCF) in any one of the switches, which constitute the VSI. The proposed fault-tolerant PM-BLDC motor drive requires fewer additional sensors and components compared to the fault-tolerant power converters, which are reported in the previous literature. Cost analysis, carried out for a 3-kW motor drive, reveals that an additional cost of only 5% is added to the raw material cost of the traditional PM-BLDC motor configuration to facilitate fault tolerance. The fault-tolerant operation of the proposed power converter is experimentally verified with a low-power laboratory prototype.

KEYWORDS

dynamic circuit reconfiguration, electric vehicles, fault-tolerant drive configurations

1 | INTRODUCTION

Electric vehicles (EVs) have assumed significance in the automobile sector owing to their capability of reducing environmental pollution and achieving conservation of energy. Penetration of EVs is mainly facilitated by the recent advancements in battery technologies, digital control platforms, power semiconductor device technologies, and high energy density permanent magnets. Permanent magnet brush-less direct current motors (or simply PM-BLDC motors) are being used in low-power EV applications due to their high efficiency, compact size (due to their high energy densities), ease of control, quiet operation, low-maintenance requirements, and high dynamic performance.[1–3]

Fault tolerance is a very important aspect of design from the standpoint of reliability for EVs. Propulsion motors in EVs are typically operated by voltage source inverters (VSIs). Thus, achieving fault tolerance against faults occurring in actuator switching devices is of paramount interest. Prior research shows that faulty power semiconductor devices contribute to as much as 38% of the total fault conditions in the drive configurations.[4] The semiconductor switch faults are categorized into two types, namely, open-circuit faults (OCFs) and short-circuit faults (SCFs).

A switched-capacitor-based multi-level boost converter configuration that can handle OCFs in the semiconductor switches is proposed in reference.[5] A multi-switch fault-tolerant drive configuration is presented by the research work reported in reference,[6] which presents the multi-switch OCF diagnosis and the corresponding reconfiguration procedure.

The fault-tolerant control operation for stator winding inter-turn failures, rotor eccentricity faults, and Hall-effect sensor failures is presented in the literature.[7–9]

For OC failures, a technique to maintain the rated output torque for a permanent magnet hybrid BLDC motor drive configuration, using field-reconstruction strategies and boosting of filed excitation, is investigated in reference.[10] Fault-tolerant torque control for a BLDC motor that can facilitate precise torque control with a reduced power dissipation despite the failure of one of its phase windings is described in reference.[11]

Fast-changing and soft commutation between the main and redundant branches of a VSI using a combination of rugged mechanical commutators and semiconductors is reported in reference.[12] The fault-tolerant analysis described in reference[12] reveals that, even though mechanical commutators are slower than power semiconductor switches, they provide the advantages of low losses, electrical isolation, and stress elimination for parallel redundant branches.

In the research work presented in reference,[13] a single-switch OC (or SC) fault-tolerant drive topology for EV applications is described, which uses six triode for alternating currents (TRIACs) and one actuator leg additionally. However, fault diagnosis algorithms were not described in this literature.

The drive topology proposed in reference[14] achieves fault-tolerant operation by adding three TRIACs to the conventional PM-BLDC motor drive. An algorithm to detect OC switch fault diagnosis is also presented in this manuscript. However, this fault-tolerant drive topology does not achieve fault tolerance against SCFs.

The power circuit configuration reported in the literature[15–18] presents a fault-tolerant strategy for OCFs in switches and the motor phase windings. This article recommends the employment of multi-phase open-end winding PM-BLDC motor (OEWBLDCM) drives for such applications, where the reliable operation of the drive is the primary concern. The work[15] also suggests some techniques to reduce the torque ripple after the occurrence of such faulty conditions. The article reported in reference[16] also explains the diagnosis algorithm for open-switch fault conditions of the multi-phase PM-BLDC motor drive configuration.

Fault-tolerant PM-BLDC motor drive topologies with a DC–DC buck converter at the front end are proposed in the literature[19,20] for magnetically suspended control moment (MSCM) gyro applications. The configuration described in reference[19] requires six additional TRIACs and an additional phase leg to achieve fault tolerance against a single-switch OCF/SCF. However, additional TRIACs, employed to achieve fault-tolerant operation, are kept in the normal (i.e., pre-fault) circuit configuration, making them susceptible to failures. While the algorithm presented in reference[19] can diagnose switch OCF/SCF conditions in the front-end buck converter and the inverter, it cannot identify the fault conditions in the additional TRIACs. The research article presented in reference[20] shows a fault-tolerant OEWBLDCM drive configuration for MSCM gyro applications. The diagnosis algorithm described in reference[20] can diagnose OCF/SCF for all the switching devices of VSI. However, this power converter configuration demands that all the motor phase windings and all the switching devices be rated for double the rated current to obtain fault-tolerant operation.

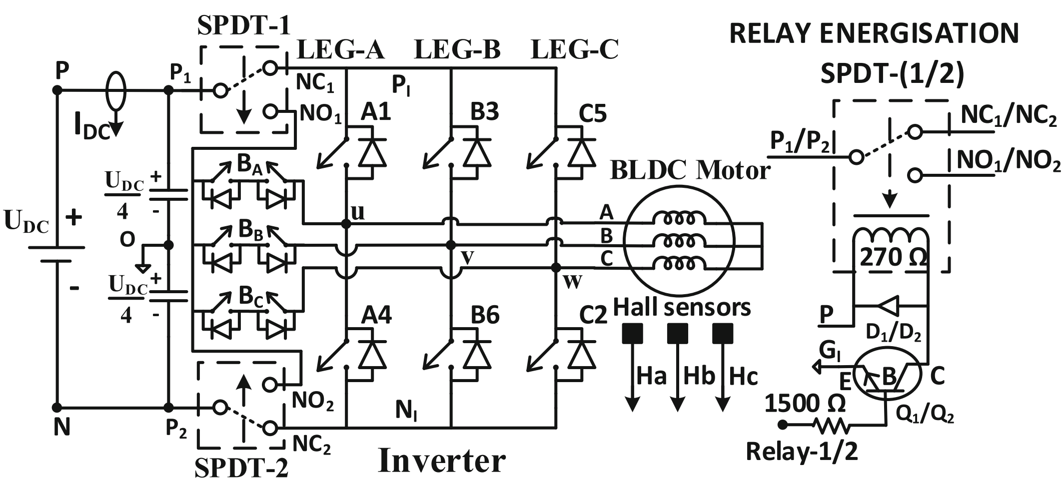

FIGURE 1 Proposed open-circuit/short-circuit fault-tolerant PM-BLDC drive configuration.

A dual-inverter-fed fault-tolerant OEWBLDCM drive for low-power EV applications is presented in reference.[21] This system is capable of diagnosing both OCF and SCF conditions in all the switching devices in the dual-inverter system.[21] In the fault-tolerant mode of operation, this topology employs two double-pole double-throw (DPDT) relays to utilize the energy stored in the healthy battery bank connected to the faulty inverter. In this system, the post-fault reconfiguration of the power converter involves a parallel reconnection of the battery banks. Thus, the effective DC input voltage to the healthy inverter is halved in the post-fault condition, restricting the post-fault power (and speed) to half the rated quantity.

This shortcoming is addressed in the configuration presented in reference,[22] wherein the supply battery bank, which is on the faulty inverter side, is reconnected in series to the supply battery bank connected to the healthy counter inverter to feed the motor. This post-fault reconnection, which needs four DPDT relays, allows the drive configuration to deliver the *rated power (speed) and torque* even after the occurrence of the fault and the subsequent circuit reconfiguration. However, this configuration requires power devices with twice the voltage rating compared to the one described in reference.[21]

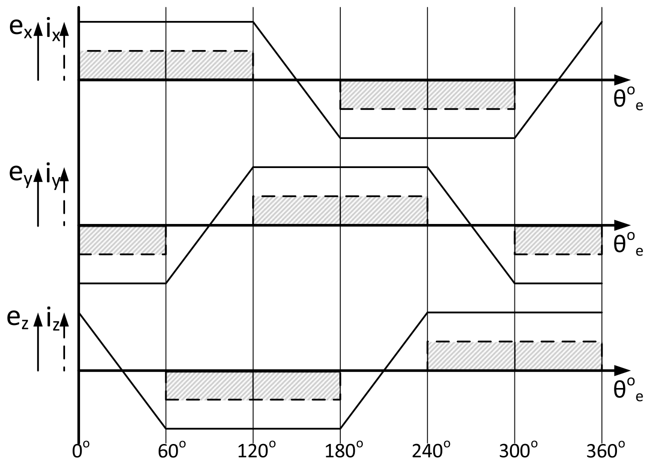

Sector-1	Sector-2	Sector-3	Sector-4	Sector-5	Sector-6
Switching scheme in normal Operating Conditions					
A1,B6	A1, C2	B3,C2	B3,A4	C5,A4	C5,B6
Switching scheme for OC/SC fault in switch A1					
B_A,B6	B_A, C2	B_B,C2	B_B,A4	B_C,A4	B_C,B6
Switching scheme for OC/SC fault in switch A4					
A1,B_B	A1, B_C	B3,B_C	B3,B_A	C5,B_A	C5,B_B

FIGURE 2 Switching logic for each sector during steady and post-fault conditions.

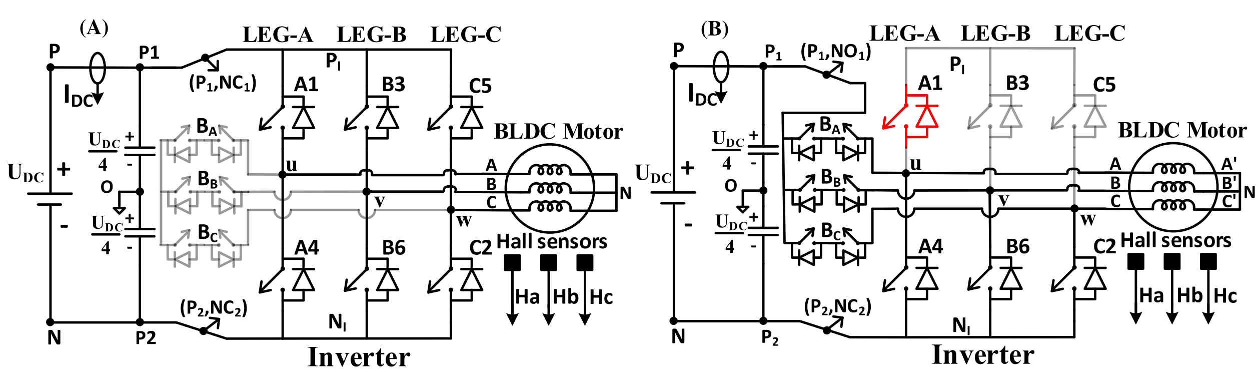

FIGURE 3 Equivalent circuit diagram of the proposed fault-tolerant drive configuration under (A) steady operation conditions and (B) open-circuit/short-circuit faulty conditions in switch “A1” (upper bank switch).

Apart from DPDT relays, the open-end winding structure-based topologies[21,22] require six voltage sensors and two current sensors for sensing the line voltages and the DC currents to diagnose the SCF and OCF conditions. Also, all the switching devices present are susceptible to the development of faults in these topologies. These shortcomings in the prior work are the motivating factors to explore new power converter configurations, which can deliver rated power to the motor even in a post-fault scenario with reduced switchgear.

This brief report proposes a fault-tolerant PM-BLDC motor drive configuration for low-power EV applications, which can deliver rated post-fault power to the motor. In this configuration, the additional auxiliary switching

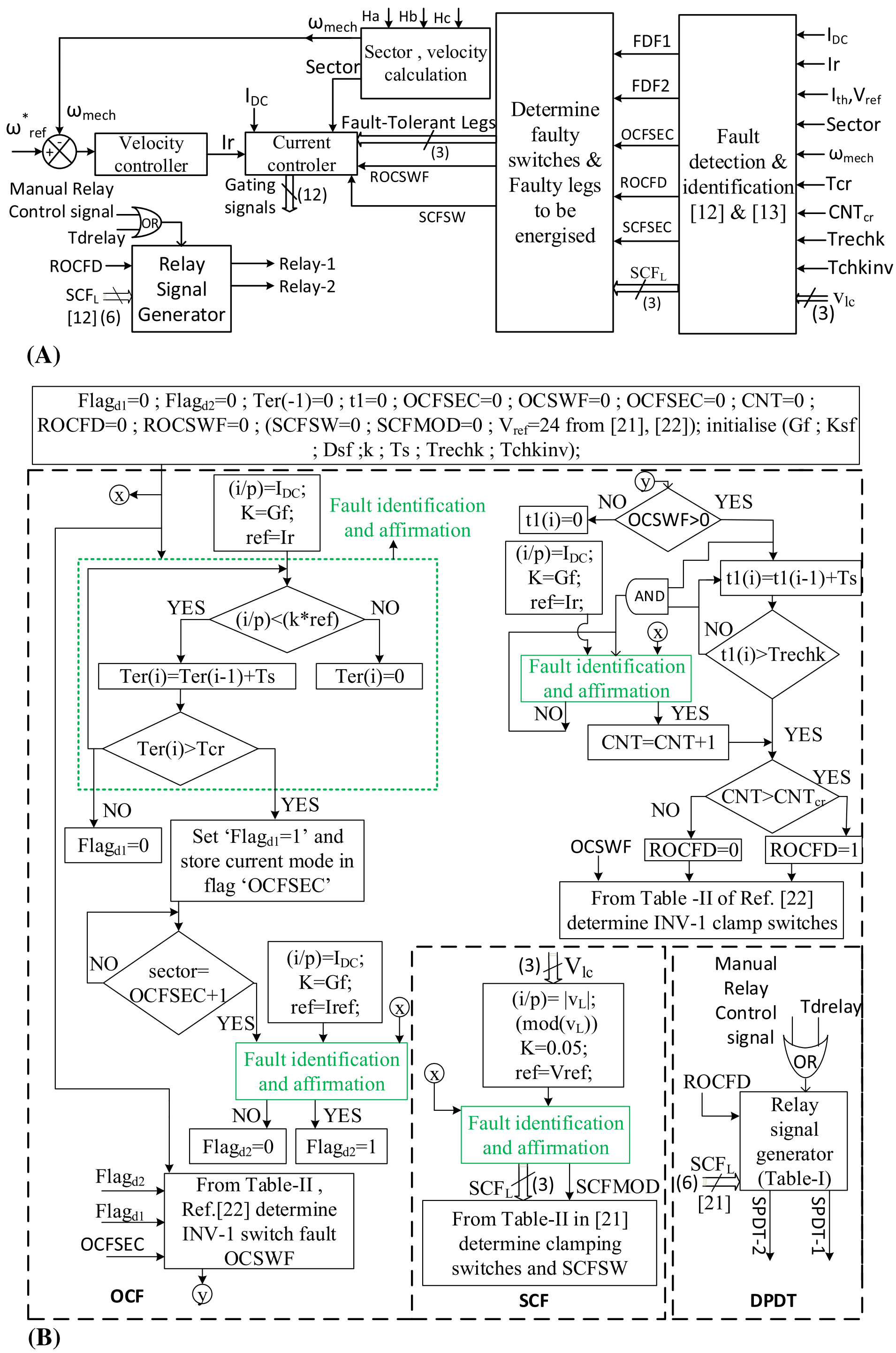

FIGURE 4 (A) Schematic presentation of fault-tolerant control mechanism. (B) Flowchart representing the fault-tolerance operation of the proposed fault-tolerant drive configuration.

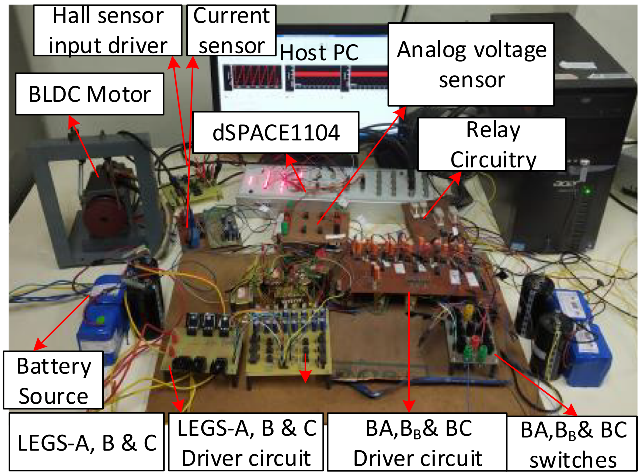

FIGURE 5 Experimental setup of the proposed fault-tolerant topologies.

TABLE 1 PM-BLDC motor parameters.

Voltage (operating)	48 V
Torque (operating)	0.6 N·m
Speed (operating)	3200 RPM
Per phase (resistance)	0.295 Ω
Back-EMF constant	11.8 V/Krpm
Power (operating)	250 W
Pole pairs	4

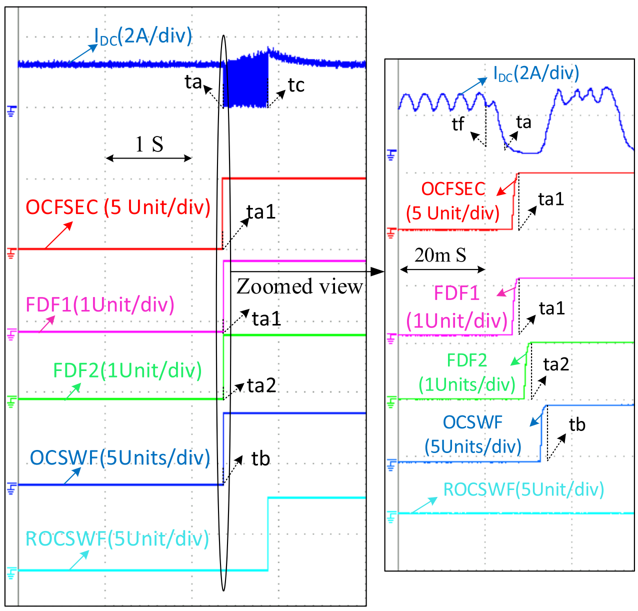

FIGURE 6 Experimental results showing the flag statuses during OCF diagnosis (for OCF in "C5") (scale: X-axis: 1-S/div; Y-axis: I_{DC} [A/div]; OCFSEC, FDF1, FDF2, OCSWF, ROCSWF [units/div]).

resources employed to implement fault tolerance are dormant in the pre-fault condition and are therefore not susceptible to the development of faults. Furthermore, this configuration requires only one current sensor and three voltage sensors to diagnose a single OCF and a single SCF, resulting in a significant drop in the additional raw material cost (RMC) to realize fault tolerance. This brief report also presents a cost analysis to prove the economic feasibility of the proposed fault-tolerant drive configuration.

2 | FAULT-TOLERANT OPERATION OF THE PROPOSED DRIVE CONFIGURATION

2.1 | Circuit description and fault-tolerant control of the PM-BLDC motor drive

Figure 1 presents the proposed fault-tolerant PM-BLDC motor drive configuration. This topological drive configuration consists of a conventional VSI with three legs (Legs “A,” “B,” and “C”). Under normal conditions, the VSI is fed with the DC power supply “U_{DC}.” Hall position sensors “Ha,” “Hb,” and “Hc” are used to sense the rotor position to generate the gating signals for the VSI. Figure 2 presents the back electromotive force (EMF), current waveforms, and inverter switching signals for all the sector positions (six sectors derived from three Hall position sensors) under steady and faulty operating conditions.

To achieve fault tolerance, the proposed topology employs three bidirectional switches “B_A,” “B_B,” and “B_C” and two single-pole double-throw (SPDT) relays “SPDT-1” and “SPDT-2.” Each of these bidirectional switches is realized by the anti-series connection of two insulated gate bipolar transistors (IGBTs) with a common emitter connection.

Before the occurrence of any fault (i.e., in the default condition), the pole terminals of the SPDT relays (“P_1” and “P_2”) respectively connect the positive and negative terminals of the input DC power supply (the battery in the case of an EV) to the corresponding terminals of the VSI through the normally closed positions “NC_1” and “NC_2,” as shown in Figures 1 and 3A.

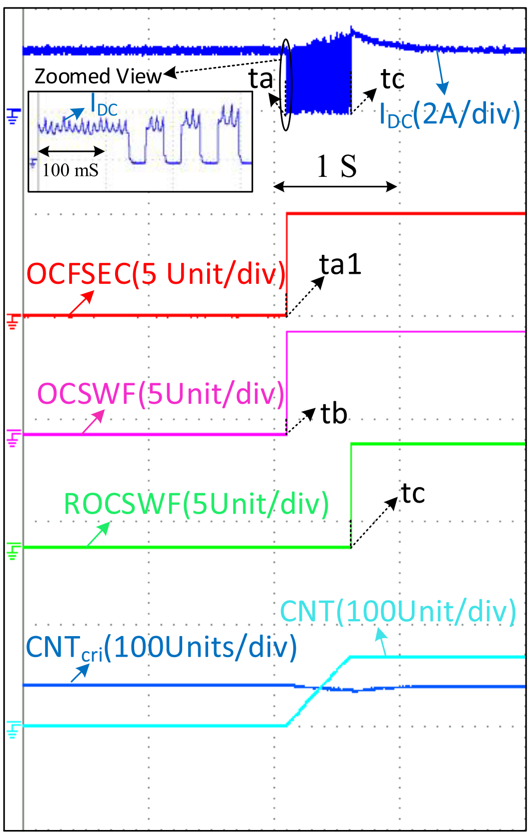

FIGURE 7 Experimental results showing the flag and counter values for OCF in “C5” (scale: X-axis: 1-S/div; Y-axis: I_{DC} [A/div]; OCFSEC, OCSWF, ROCSWF, CNT, CNT_{cri} [units/div]).

Whenever a fault (it can be either an OCF or an SCF) is detected in the three top switches (A_1, B_3, or C_5), the relay SPDT-1 is operated. This makes the pole P_1 changeover from the default position NC_1 to the normally open contact, NO_1. This changeover connects the common end of the bidirectional switches "B_A," "B_B," and "B_C" to the positive terminal of the battery through the pole P_1 of SPDT-1. At the same time, all three bidirectional switches "B_A," "B_B," and "B_C" are gated and the gating signals for all the three top switches (A_1, B_3, and C_5) are withdrawn. With this maneuver, the bidirectional switches "S_A," "S_B," and "S_C" replace the three top switches and the drive continues to operate normally despite the development of the fault, delivering full power to the motor (Figure 3B). It is obvious that a similar operation is achievable when a fault occurs in one of the three bottom switches. In this case, the relay SPDT-2 is operated, making the pole P_2 to changeover from the default position NC_2 to NO_2, connecting the common end of the bidirectional switches "B_A," "B_B," and "B_C" to the battery negative terminal. Thus, it is not necessary to energize the relays in the default condition, which is an advantageous proposition.

It may also be noted that, while an OEWBLDCM drive requires six voltage sensors and two current sensors to implement fault tolerance, the proposed topology needs only three voltage sensors and one current sensor with the same number of power semiconductor switches. In a scenario, wherein the cost of sensors dominates the cost of semi-conductors, this topological configuration brings in a considerable saving in the RMC to implement the fault-tolerance feature. Also, the proposed topological configuration requires lesser supporting switchgear to implement 100% fault tolerance. Only two SPDT relays are needed in this topology as compared to four DPDT relays in reference,[13] which is another contributing factor to the reduction in the RMC. Furthermore, all the three additional bidirectional switches are dormant in the pre-fault condition; hence, they are not susceptible to the development of faults (Figure 3A).

The fault tolerance of the proposed PM-BLDC motor drive configuration is verified for both open-loop and closed-loop drive control operations. The closed-loop control operation is performed by a conventional outer velocity controller and an inner current controller. Figure 4A represents the overview of the presented closed-loop drive control with the fault-tolerance feature.

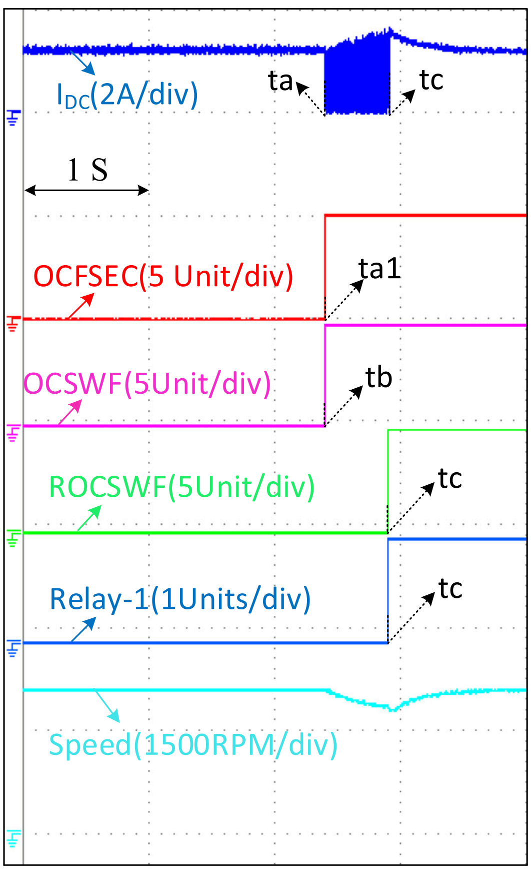

FIGURE 8 Experimental results showing the fault-tolerant operation (open loop) for OCF in "C5" (scale: X-axis: 1-S/div; Y-axis: I_{DC} [A/div]; OCFSEC, OCSWF, ROCSWF, Relay-1 [units/div]; speed [RPM/div]).

2.2 | Fault diagnosis control for the proposed drive configuration

The OCF and SCF diagnosis algorithms, which had earlier been proposed for an open-end winding PM-BLDC motor drive,[12] have been adopted in the proposed topology, which is briefly recapitulated below:

1. The diagnosis of the OCF is accomplished by the identification of interruption in the input DC current. If this current is interrupted for a pre-specified critical time period, the OCF is asserted, the corresponding sector is identified, and its number is stored in a flag named "OCFSEC." Two more flags "FDF1" and "FDF2" are set to unity if the interruption of the DC current is affirmed in the present sector and the immediately succeeding sector. Based on the status of these flags, the switch responsible for the fault is identified, and the faulty switch number is noted in the given flag named "OCSWF."[12]
2. The diagnosis of the SCF is accomplished by the identification of the zero-voltage periods in line voltages, which are sensed during the non-conducting period of 60° between the top and the bottom of the switching devices in any given phase leg. The sector in which the zero-voltage period in a given line voltage is observed is stored in the flag "SCFSEC." Based on this information, the SCF is identified, and its corresponding switch number is noted in the flag named "SCFSW."[12]

The overall fault-tolerant operation of the proposed drive configuration is shown in Figure 4B.

3 | RESULTS AND DISCUSSION

Figure 5 presents the experimental prototype, which is used to validate the fault-tolerant capability of the proposed drive configuration using the dSPACE 1104 control platform. Table 1 presents the parameters of the PM-BLDC machine

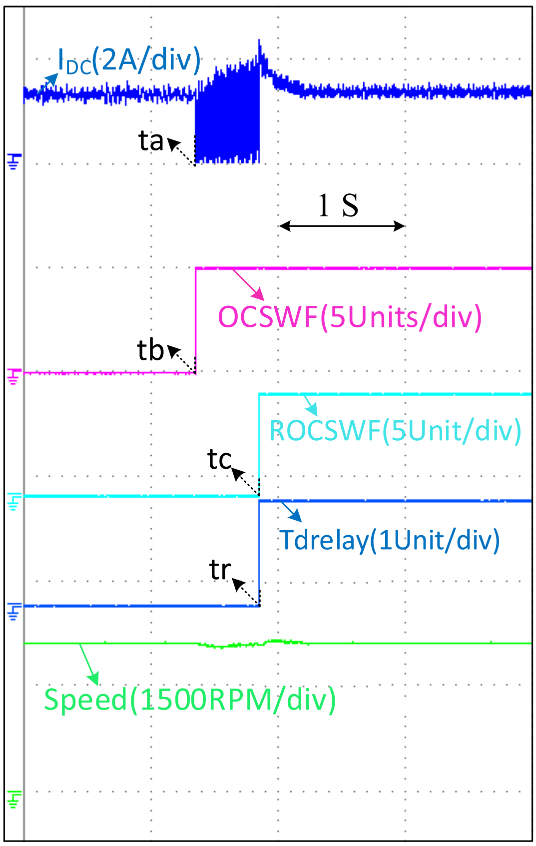

FIGURE 9 Experimental results showing the fault-tolerant operation (closed loop) for OCF in "C5" (scale: X-axis: 1-S/div; Y-axis: I_{DC} [A/div]; OCSWF, ROCSWF, Tdrelay [units/div]; speed [RPM/div]).

used in the experimental prototype. To emulate the occurrence of OCF and SCF experimentally, the gating signal for one of the switches is either withdrawn fully or maintained continuously.

The experimental validation for the fault-tolerant operation of the presented topology for the OCF is presented in Figures 6–9. With the enforcement of OCF in switch "C5" (at instant "tf"; Figure 6), the diagnosis is carried out through the flags "OCFSEC," "FDF1," and "FDF2" (at instants "ta1" and "ta2"; Figure 6). Based on this information, the actuator switch number corresponding to the OCF is noted in the flag "OCSWF" (at the instant "tb"; Figures 6–8). To conclusively assert the occurrence of the OCF, a counter "CNT" is triggered at this point of time, which counts the number of the zero-current periods in the probation period (tc − tb). Only when this count exceeds a critical count, the fault is finally asserted and the value stored in the flag "OCSWF" is transferred to the final flag "ROCSWF,"[13] which initiates the post-fault circuit reconfiguration procedure. Figure 9 validates the fault tolerance against the OCF in switch "C5" for the closed-loop drive operation.

Figure 10 illustrates the experimental verification against the SCF for the proposed drive configuration. In this experiment, the gating signal for switch A4 is held continuously high. With the diagnosis control algorithm described in reference,[12] the SCF is diagnosed and the switch number of the faulty switch is noted in the given flag "SCFSW" (at the time instant "ty"; Figure 10). As the number of the faulty switch belongs to the lower bank of the VSI, SPDT-2 is energized using Relay-2 (Figure 1) at the instant "ty," as shown in Figure 10. With the reconfiguration procedure explained in Section 2, the drive can perform normally and eventually attains its rated speed even after the occurrence of the SCF in the switch A4.

4 | FEASIBILITY ANALYSIS OF THE PROPOSED DRIVE CONFIGURATION

Table 2 summarizes the comparison of the presented fault-tolerant PM-BLDC motor drive configuration vis-à-vis the configurations reported in the previous literature. Table 3 shows the additional RMC incurred for the fault-tolerant

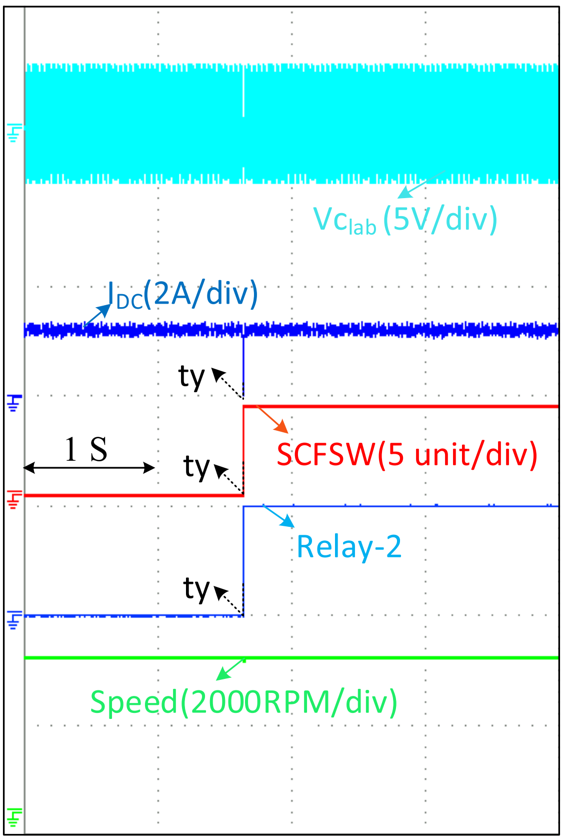

FIGURE 10 Experimental results showing the drive fault control operation during SCF in "A4" (scale: X-axis: 1-S/div; Y-axis: VC_{lab} [V/div], I_{DC} [A/div]; SCFSW, Relay-2 [units/div]; speed [RPM/div]).

TABLE 2 Comparison of configuration proposed with the prior art literature.

Features of the drive configuration	Configuration[14]	Configuration[19]	Configuration[20]	Configuration[21]	Configuration[22]	Proposed configuration
(1) Isolated DC source requirement	No	No	No	Yes	Yes	No
(2) Actuator switches	6 switches (traditional) and 3 TRIACs	6 switches (traditional) and 6 TRIACs and additional 1 leg (2 switches)	12 switches	12 switches	12 switches	12 switches
(3) Ratings of switching devices	Rated motor current and voltage	Rated motor current and voltage	Double the rated motor current and rated motor voltage	Rated motor current and half the rated voltage	Rated current and voltage	All switches Motor rated current and 6 switches (half the rated voltage) and 6 switches (rated voltage)
(4) PM-BLDC motor design ratings	Operating current and voltage	Operating current and voltage	Operating voltage and 2× (operating current)	Operating current and voltage	Operating current and voltage	Operating current and voltage
(5) Diagnosis and tolerance of switch fault	OCF only	OCF and SCF	OCF and SCF	OCF and SCF	OCF and SCF	OCF and SCF
(6) Fault diagnosis in additional switches of the inverter	Not susceptible to faults	No	Yes	Yes	Yes	Not susceptible to faults
(7) Maximum speed, torque, and power during post fault	Rated power, rated torque, and rated speed	Rated power, rated torque, and rated speed	Rated power, rated torque, and rated speed	Rated torque and half the rated power and speed	Rated power, torque, and speed	Rated torque and half the rated power and speed
(8) Auxiliary components	No	3 switches, buck converter, and 1 fault-tolerant leg	1 SPDT relay, buck converter, and 1 fault-tolerant leg	2 DPDT relays	4 DPDT relays	2 SPDT relays
(9) Applicability for EV applications	Yes	No	No	Yes	Yes	Yes

TABLE 3 Cost evaluation of fault-tolerant drive configurations (Indian Rs.).

Name of the component			Unit price (Rs./-)	Number of units	Total price (Rs./-)
(a) PM-BLDC motor drive 3 KW, 96 V			31,790	1	31,790
(b) Batteries (lithium ion) (720 WH, 60 AH, and 12 V)			13,630	8	109,040
(c) Actuator switches along with driver circuitry (safety factor for voltage and current considered as 2)		(c_1) Configuration[21]	(65 + 309)	12	4488
		(c_2) Configuration[22]	(158 + 309)	12	5604
		(c_3) Proposed configuration	(158 + 65) + (309)	(6, 6) (9)	4119
		(c_4) Traditional inverter	(158 + 309)	6	2802
(d) Sensors	Current sensors	(d_1) Topologies[21,22]	1880	2	3760
		(d_2) Proposed configuration	1880	1	1880
	Analog voltage sensors required (TL084CN and ISO-124)[21]	(d_3) Topologies[21,22]	(895 + 13)	6 (ISO-124) 2 (TL084CN)	5396
		(d_4) Proposed configuration	(895 + 13)	3 (ISO-124) 1 (TL084CN)	2698
(e) Auxiliary devices (DPDT[21,22]; SPDT [proposed configuration] relays)		(e_1) Configuration[21]	808	2	1616
		(e_2) Configuration[22]	808	4	3232
		(e_3) Proposed configuration	345	2	690

Additional price (in %) incurred for the open-circuit/short-circuit fault-tolerant configuration[21] with respect to the conventional PM-BLDC drive $= \left[\frac{d_3+e_1+[c_1-c_4]+d_1}{a+b+c_4}\right] * 100\% = \left[\frac{5396+1616+1686+3760}{31,790+109,040+2802}\right] * 100\% = 8.67\%$

Additional price (in %) incurred for the open-circuit/short-circuit fault-tolerant configuration[22] with respect to the conventional PM-BLDC drive $= \left[\frac{d_3+e_2+[c_2-c_4]+d_1}{a+b+c_4}\right] * 100\% = \left[\frac{5396+3232+2802+3760}{31,790+109,040+2802}\right] * 100\% = 10.57\%$

Additional price (in %) incurred for the proposed open-circuit/short-circuit fault-tolerant configuration with respect to the conventional PM-BLDC drive $= \left[\frac{d_4+e_3+[c_3-c_4]+d_2}{a+b+c_4}\right] * 100\% = \left[\frac{2698+690+1875+1880}{31,790+109,040+2802}\right] * 100\% = 4.97\%$

configurations with respect to the traditional drive configuration. The cost evaluation presented in Table 3 shows that the proposed drive configuration incurs only 5% additional RMC, while the OEWBLDC motor drives reported in the literature[21,22] respectively incur 9% and 11%. This confirms the economic viability of the drive configuration for EV applications, with a post-fault delivery of 100% rated power.

5 | CONCLUSION

This paper presented a fault-tolerant PM-BLDC motor drive topology for low-power EV applications. This power converter uses three bidirectional power devices, which are inactive in the normal mode of operation, enhancing its reliability. The proposed power converter, upon diagnosing an OCF/SCF in any one of the switching devices of the VSI, automatically reconfigures itself by inserting these bidirectional switching devices to achieve the feature of fault tolerance. Cost analysis reveals that the proposed topology, owing to its employment of fewer current and voltage sensors (compared with the previous topologies reported), adds only 5% additional RMC to add the fault-tolerance feature to the traditional PM-BLDC motor drive topology and offers a price-competent solution.

DATA AVAILABILITY STATEMENT

The data that support the findings of this study are available within the article and also in appropriate references.

ORCID

Patnana Hema Kumar https://orcid.org/0000-0002-3411-1847
Suresh Lakhimsetty https://orcid.org/0000-0001-5811-4519

REFERENCES

1. Krishnan R. *Permanent Magnet Synchronous and Brushless DC Motor Drives*. 1st ed. CRC Press, Ch. 1; 2010:50-51.
2. Chan CC. An overview of electric vehicle technology. *Proc IEEE*. 1993;81(9):1202-1213. doi:10.1109/5.237530
3. Chan CC, Chau KT, Jiang JZ, Xia W, Zhu M, Zhang R. Novel permanent magnet motor drives for electric vehicles. *IEEE Trans Ind Electron*. 1996;43(2):331-339. doi:10.1109/41.491357
4. Fuchs FW. Some diagnosis methods for voltage source inverters in variable speed drives with induction machines—a survey. IECON 29th Annual Conference of the IEEE Industrial Electronics Society vol. 2. Roanoke, VA, USA. November 2003:1378-1385.
5. Ajaykumar T, Patne NR. Fault-tolerant switched capacitor–based boost multilevel inverter. *Int J Circ Theor Appl*. 2019;47:1615-1629.
6. Kumar PH, Somasekhar VT. An enhanced fault-tolerant and auto-reconfigurable BLDC motor drive for electric vehicle applications. *IEEE J Emerging Sel Top Ind Electron*. 2022;4(1):368-380.
7. Shakouhi M, Mohamadian M, Afjei E. Fault-tolerant control of brushless DC motors under static rotor eccentricity. *IEEE Trans Ind Electron*. 2015;62(3):1400-1409. doi:10.1109/TIE.2014.2365439
8. Jafari A, Faiz J, Jarrahi MA. A simple and efficient current-based method for interturn fault detection in BLDC motors. *IEEE Trans Industr Inform*. 2021;17(4):2707-2715. doi:10.1109/TII.2020.3009867
9. Ebadpour M, Amiri N, Jatskevich J. Fast fault-tolerant control for improved dynamic performance of Hall-sensor-controlled brushless DC motor drives. *IEEE Trans Power Electron*. 2021;36(12):14051-14061. doi:10.1109/TPEL.2021.3084921
10. Liu C, Chau KT, Li W. Comparison of fault-tolerant operations for permanent-magnet hybrid brushless motor drive. *IEEE Trans Magn*. 2010;46(6):1378-1381. doi:10.1109/TMAG.2010.2042928
11. Aghili F. Fault-tolerant torque control of BLDC motors. *IEEE Trans Power Electron*. 2011;26(2):355-363. doi:10.1109/TPEL.2010.2060361
12. Cordeiro A, Palma J, Maia J, Resende M. Combining mechanical commutators and semiconductors in fast changing redundant inverter topologies. IEEE EUROCON - International Conference on Computer as a Tool, vol. 2011, April 2011:1-4.
13. Errabelli RR, Mutschler P. Fault-tolerant voltage source inverter for permanent magnet drives. *IEEE Trans Power Electron*. 2012;27(2): 500-508. doi:10.1109/TPEL.2011.2135866
14. Park B, Lee K, Kim R, Kim T, Ryu J, Hyun D. Simple fault diagnosis based on operating characteristic of brushless direct-current motor drives. *IEEE Trans Ind Electron*. 2011;58(5):1586-1593. doi:10.1109/TIE.2010.2072895
15. Villani M, Tursini M, Fabri G, Castellini L. High reliability permanent magnet brushless motor drive for aircraft application. *IEEE Trans Ind Electron*. 2012;59(5):2073-2081. doi:10.1109/TIE.2011.2160514
16. Kim YH, Heo HJ, Park JH, Kim JM. Fault tolerant control methods for dual type independent multi-phase BLDC motor under the open-switch fault conditions. *J Electr Eng Technol*. 2018;13(2):722-732.
17. Khan KR, Miah MS. Fault-tolerant BLDC motor-driven pump for fluids with unknown specific gravity: an experimental approach. *IEEE Access*. 2020;8:30160-30173.
18. Salehifar M, Arashloo RS, Moreno-Equilaz JM, Sala V, Romeral L. Fault detection and fault tolerant operation of a five phase PM motor drive using adaptive model identification approach. *IEEE J Emerg Sel Topics Power Electron*. 2014;2(2):212-223. doi:10.1109/JESTPE.2013.2293518
19. Li H, Li W, Ren H. Fault-tolerant inverter for high-speed low-inductance BLDC drives in aerospace applications. *IEEE Trans Power Electron*. 2017;32(3):2452-2463. doi:10.1109/TPEL.2016.2569611
20. Feng J, Liu K, Wang Q. Scheme based on buck-converter with three-phase H-bridge combinations for high-speed BLDC motors in aerospace applications. *IET Electr Power Appl*. 2018;12(3):405-414. doi:10.1049/iet-epa.2017.0615
21. Kumar PH, Lakhimsetty S, Somasekhar VT. An open-end winding BLDC motor drive with fault diagnosis and auto reconfiguration. *IEEE J Emerg Sel Top Power Electron*. 2020;8(4):3723-3735. doi:10.1109/JESTPE.2019.2948968
22. Patnana HK, Veeramraju Tirumala S. A cost-effective and fault-tolerant brushless direct current drive with open-stator windings for low power electric vehicles. *Int J Circ Theor Appl*. 2021;49(9):2885-2908. doi:10.1002/cta.3048

How to cite this article: Kumar PH, Lakhimsetty S, Somasekhar VT. A low-cost fault-tolerant permanent magnet brush-less direct current motor drive for low-power electric vehicle applications. *Int J Circ Theor Appl*. 2023;51(9):4442-4453. doi:10.1002/cta.3642